FEBS Letters 584 (2010) 4344–4350

journal homepage: www.FEBSLetters.org

# Sequence discrimination of the Zα domain of human ADAR1 during B–Z transition of DNA duplexes

Yeo-Jin Seo [a,1], Hee-Chul Ahn [b,1], Eun-Hae Lee [a,1], Jongchul Bang [c], Young-Min Kang [a], Hee-Eun Kim [a], Yeon-Mi Lee [a], Kyungmin Kim [d], Byong-Seok Choi [c,*], Joon-Hwa Lee [a,*]

[a] Department of Chemistry, RINS, and Environmental Biotechnology National Core Research Center, Gyeongsang National University, Jinju, Gyengnam 660-701, Republic of Korea
[b] Advanced Analysis Center, KIST, Seoul 130-650, Republic of Korea
[c] Department of Chemistry, KAIST, Daejeon 305-701, Republic of Korea
[d] Department of Molecular Cell Biology, Sungkyunkwan University School of Medicine, Suwon, Gyeonggi 440-746, Republic of Korea

ARTICLE INFO

*Article history:*
Received 17 August 2010
Revised 14 September 2010
Accepted 20 September 2010
Available online 26 September 2010

Edited by Gianni Cesareni

*Keywords:*
NMR
Z-DNA
Hydrogen exchange
Z-DNA binding protein
B–Z transition
Non-CG repeat DNA

ABSTRACT

**The Zα domain of human ADAR1 ($Z\alpha_{ADAR1}$) preferentially binds Z-DNA rather than B-DNA with high binding affinity. $Z\alpha_{ADAR1}$ binds to the Z-conformation of both non-CG-repeat DNA duplexes and a $d(CGCGCG)_2$ duplex similarly. We performed NMR experiments on complexes between the $Z\alpha_{ADAR1}$ and non-CG-repeat DNA duplexes, $d(CACGTG)_2$ or $d(CGTACG)_2$, with a variety of protein-DNA molar ratios. Comparison of these results with those from the analysis of $d(CGCGCG)_2$ in the previous study suggests that $Z\alpha_{ADAR1}$ exhibits the sequence preference of $d(CGCGCG)_2 \gg d(CACGTG)_2 > d(CGTACG)_2$ through multiple sequence discrimination steps during the B–Z transition.**


## 1. Introduction

Left-handed Z-DNA is in a higher energy conformation than right-handed B-DNA and forms in a polymer of alternating pyrimidine–purine nucleotides under high salt conditions [1–3]. Z-DNA is stabilized by negative supercoiling generated by transcription *in vivo* [2,3] or by complex formation with the Z-DNA binding proteins [4–10]. The most favourable sequence for Z-DNA formation is an alternating d(CG)-repeat, with the dC in the *anti*-conformation and the dG in the unusual *syn*-conformation [1–3], which causes the backbone to follow a zigzag path [2,3]. The B–Z transition involves each base-pair (bp) flipping upside down [11]. During this process, the base of each dG inverts into the *syn*-conformation, whereas each dC remains in the *anti*-conformation because both the sugar and base flip over [11].

Human ADAR1 deaminates adenine in pre-mRNA to yield inosine, which codes as a guanine [4]. The Zα domain of human ADAR1 ($Z\alpha_{ADAR1}$) preferentially binds Z-DNA rather than B-DNA with high binding affinity [12–14]. The crystal structure of a $Z\alpha_{ADAR1}$–Z-DNA complex revealed that two Zα domains bind to each strand of double-stranded DNA with twofold symmetry with respect to the DNA helical axis [4]. A previous NMR study on a $d(CGCGCG)_2$–$Z\alpha_{ADAR1}$ complex [15] suggests the *active-mono* B–Z transition mechanism of a 6-bp DNA duplex (Fig. 1), in which (*i*) one molecule of $Z\alpha_{ADAR1}$ (denoted as **P**) binds directly to the B-form DNA (denoted as **B**); (*ii*) the B–Z transition of DNA in the complex follows; and (*iii*) finally, the stable $\mathbf{ZP_2}$ complex (the Z-form DNA denoted as **Z**) is produced by the addition of another **P**.

Z-DNA can also be formed in double-stranded DNA sequences that lack alternating pyrimidine–purine base pairs or that include A·T base pairs [16–18]. The A·T base pairs partially distort the overall Z-DNA structure by disrupting the hydration spine [16]. The ability of DNA duplexes to undergo the B–Z transition can be ordered as follows: (*i*) d(CG) repeat (which undergoes the transition most readily), (*ii*) d(TG/AC) repeat, (*iii*) d(GGGC) repeat, and (*iv*) d(TATA) repeat [19,20]. Recently, a structural study revealed that $Z\alpha_{ADAR1}$ binds to the Z-conformation of both non-CG-repeat DNA duplexes and a $d(CGCGCG)_2$ duplex similarly, suggesting that $Z\alpha_{ADAR1}$ recognizes Z-DNA through a common structural feature rather than by a specific sequence or structural alternations [21].

* Corresponding authors. Fax: +82 42 350 8120 (B.-S. Choi); +82 55 761 0244 (J.-H. Lee).
*E-mail addresses:* byongseok.choi@kaist.ac.kr (B.-S. Choi), joonhwa@gnu.ac.kr (J.-H. Lee).
[1] These authors contributed equally to this work.

0014-5793/$36.00 
doi:10.1016/j.febslet.2010.09.036

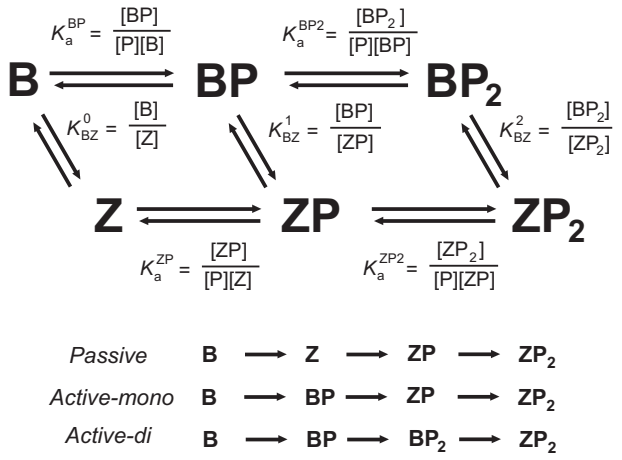


**Fig. 1.** B–Z transition of a 6-bp DNA duplex by two $Z\alpha_{ADAR1}$ proteins. **B** and **Z** indicate the B-form and Z-form of the DNA duplex and **P** indicates $Z\alpha_{ADAR1}$.

However, the detailed molecular mechanism responsible for how $Z\alpha_{ADAR1}$ discriminates between DNA sequences and then selectively recognizes the alternating $d(CG)_n$ sequence in a long genomic DNA is not well understood.

To investigate the effect of DNA duplex sequence on the binding affinity and B–Z conversion activity of $Z\alpha_{ADAR1}$, we have performed NMR experiments on complexes between $Z\alpha_{ADAR1}$ and the non-CG-repeat DNA duplexes, $d(CACGTG)_2$ [referred to as CA6] or $d(CGTACG)_2$ [referred to as TA6], (Fig. 2A) with a variety of protein-to-DNA (*P*/*N*) molar ratios. Comparison of these results with those from experiments using $d(CGCGCG)_2$ [refered to as CG6], which were previously reported [15], lead to valuable insights into the molecular mechanism of the sequence discrimination exhibited by $Z\alpha_{ADAR1}$ when it induces the B–Z transition.

## 2. Materials and methods

### 2.1. Sample preparation

The DNA oligomers, d(CACGTG) and d(CGTACG), were purchased from M-biotech Inc. (Seoul, Korea). The oligomers were purified by reverse-phase HPLC and desalted using a Sephadex G-25 gel filtration column. The amounts of the DNA samples were represented as the concentration of DNA duplexes which was a half of that of single-stranded DNA. To produce $^{15}N$-labelled $Z\alpha_{ADAR1}$, BL21(DE3) bacteria were grown in M9 medium containing 1 g/l $^{15}NH_4Cl$. Expression and purification of $^{15}N$-labelled $Z\alpha_{ADAR1}$ has been described in the previous report [8]. The protein concentration was measured spectroscopically using an extinction coefficient of 6970 $M^{-1}$ $cm^{-1}$ at 280 nm. The DNA duplexes, CA6 and TA6, and protein samples were dissolved in a 90% $H_2O$/10% $D_2O$ NMR buffer containing 10 mM sodium phosphate (pH 8.0) and 100 mM NaCl.

### 2.2. NMR experiment

All $^1H$ and $^{15}N$ NMR experiments were performed on a Varian 900 MHz spectrometer (KIST, Seoul) equipped with triple resonance probe. All $^1H$ and $^{15}N$ NMR spectra were obtained using the complex samples which were prepared by the addition of $^{15}N$-labelled $Z\alpha_{ADAR1}$ to 0.2 mM DNA samples in a NMR buffer at the indicated *P*/*N* ratio. One dimensional (1D) NMR data were processed with either the program VNMRJ (Varian, Palo Alto) or FELIX2004 (Accelrys, San Diego), whereas 2D data were processed with the program NMRPIPE [22] and analyzed with the program Sparky [23]. External 2-2-dimethyl-2-silapentane-5-sulfonate was used for the $^1H$ and $^{15}N$ references.

### 2.3. Hydrogen exchange rate measurement

The The apparent longitudinal relaxation rate constants ($R_{1a} = 1/T_{1a}$) of the imino protons of free DNA and the DNA–$Z\alpha_{ADAR1}$ complexes at various *P*/*N* ratios were determined by semi-selective inversion recovery 1D NMR experiments. The apparent relaxation rate constant of water ($R_{1w}$) was determined by a selective inversion recovery experiment, using a DANTE sequence for selective water inversion [24]. $R_{1a}$ and $R_{1w}$ were determined by curve fitting of the inversion recovery data to the appropriate single-exponential function. The hydrogen exchange rate constants ($k_{ex}$) of the imino protons were measured by a water magnetization transfer experiment. The intensities of each imino proton were measured

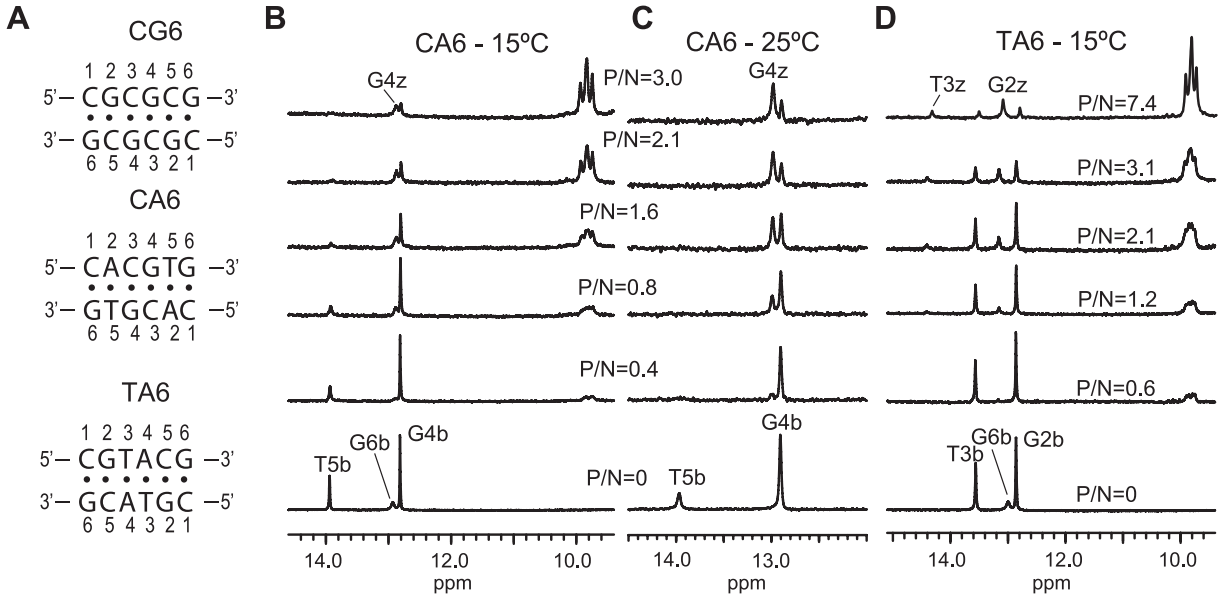


**Fig. 2.** (A) Sequence contexts of the DNA duplexes. (B) 1D imino proton spectra of the CA6 duplex in NMR buffer at 15 °C and (C) 25 °C upon titration with $Z\alpha_{ADAR1}$. (D) 1D imino proton spectra of the TA6 duplex in NMR buffer at 15 °C upon titration with $Z\alpha_{ADAR1}$.

with 20 different delay times. The $k_{ex}$ for the imino protons were determined by fitting the data to Eq. (1):

$$\frac{I_0 - I(t)}{I_0} = 2\frac{k_{ex}}{(R_{1w} - R_{1a})}(e^{-R_{1a}t} - e^{-R_{1w}t}) \quad (1)$$

where $I_0$ and $I(t)$ are the peak intensities of the imino proton in the water magnetization transfer experiments at times zero and $t$, respectively, and $R_{1a}$ and $R_{1w}$ are the apparent longitudinal relaxation rate constants for the imino proton and water, respectively, measured in semi-selective inversion recovery 1D NMR experiments [24,25].

### 2.4. Isothermal titration calorimetry (ITC) experiments

Measurements of association constants were performed at specific temperatures (CG6: 35 °C, CA6: 25 °C, TA6: 15 °C) on a MicroCal VP-ITC calorimeter (Northhampton, MA). In a typical experiment, 1.5 ml of 0.02 mM $Z\alpha_{ADAR1}$ in a buffer containing 10 mM sodium phosphate (pH 8.0) and 100 mM NaCl were titrated using a 0.10 mM DNA duplex samples in the same buffer (25 injections of 10 μl each). The results were analyzed using Origin 7.0 (OriginLab Co., Northhampton, MA).

## 3. Results and discussion

### 3.1. Titration of $Z\alpha_{ADAR1}$ to non-CG-repeat DNA duplexes

All imino resonances of CA6 and TA6 disappeared at 35 °C (Supplementary material Fig. S7), indicating that these two DNA duplexes are very unstable as compared to CG6; thus, all NMR experiments were conducted at 15 or 25 °C. Interestingly, the G6b imino proton resonances in the both free CA6 and TA6 duplexes could be observed 1D imino proton spectra acquired at 900 MHz field at 15 °C (Fig. 2B and D), even though the C1·G6 base pairs are the terminal base pair of the very short (six base-paired) DNA duplexes. However, at 600 MHz field, these resonances are too line-broadened to be observed at the same temperature (*data not shown*). Fig. 2B and D show the change of the imino proton spectra of CA6 and TA6 upon the titration with $Z\alpha_{ADAR1}$ at 15 °C. The new resonances [G4z of CA6; G2z and T3z of TA6] are indicative of the Z-form helix induced by $Z\alpha_{ADAR1}$. Surprisingly, the G4z and T5z imino proton resonances are extensively line-broadened or not observed in the CA6–$Z\alpha_{ADAR1}$ complex at 15 °C (Fig. 2B), indicating that the Z-form helix of the CA6–$Z\alpha_{ADAR1}$ complex exhibits the unusual dynamic property compared to the CG6–$Z\alpha_{ADAR1}$ or TA6–$Z\alpha_{ADAR1}$ complexes. However, the G4z imino proton resonances in the CA6–$Z\alpha_{ADAR1}$ complex became more sharpened in the 1D NMR spectra as temperature increased to 25 °C (Fig. 2C). Fig. 3 shows the fractions of Z-DNA ($f_Z$) within total DNA populations of the CA6 (25 °C) and TA6 (15 °C) duplexes complexed with $Z\alpha_{ADAR1}$, which were determined by the integration of new resonances as a function of the $P/N$ ratio. Only about 76% of the TA6 duplexes were converted to Z-DNA by $Z\alpha_{ADAR1}$ even though the $P/N$ ratio was increased to 7.4 (Fig. 2D), whereas most of the CG6 sequences exhibited the Z-conformation at a $P/N$ ratio $\geqslant$ 2.0 [15]. In the case of CA6, about 89% of the DNA duplexes displayed the Z-conformation at a $P/N$ ratio = 5.3 (Fig. 3). This result indicates that the non-CG-repeat DNA duplexes have lower binding affinities for $Z\alpha_{ADAR1}$ than does an alternating $d(CG)_n$ DNA duplex.

### 3.2. Exchange rate constants of imino protons of the CA6 and TA6 duplexes

The hydrogen exchange rate constants ($k_{ex}$) for the imino protons of free and $Z\alpha_{ADAR1}$–bound CA6 and TA6 at various $P/N$ ratios were determined at 15 and/or 25 °C by the water magnetization transfer method (see Fig. 4) [24–28]. The protein binding to DNA duplex could change the rate constant and/or the equilibrium constant for base-pair opening (see Supplementary material). Thus the hydrogen exchange data can be used to probe how intramolecular or intermolecular interactions stabilize nucleic acid duplexes. The G4b and T5b of free CA6 have $k_{ex}$ values of 39.2 ± 0.6 and 86.2 ± 2.4 $s^{-1}$ at 25 °C, respectively. Fig. 4C shows $k_{ex}$ data for the G4b of the CA6–$Z\alpha_{ADAR1}$ complex, for which the $k_{ex}$ decreased to 18.6 ± 3.7 $s^{-1}$ as the $f_Z$ was increased to 0.89 (meaning that the $P/N$ ratio increased from 0 to 5.3). The G2b and T3b of free TA6 have $k_{ex}$ values of 11.5 ± 0.5 and 11.4 ± 0.4 $s^{-1}$ at 15 °C, respectively. Interestingly, the $k_{ex}$ of the G2b in the TA6–$Z\alpha_{ADAR1}$ complex increased to 19.3 ± 3.6 $s^{-1}$ as the $f_Z$ was increased to 0.76 (Fig. 4D). The imino protons of the Z-form were more slowly exchanged than those of the B-form (Fig. 4). In contrast to results obtained for CG6 in the previous study [15], clear changes in the $k_{ex}$ values of the G2z in the TA6–$Z\alpha_{ADAR1}$ complex and the G4z in the CA6–$Z\alpha_{ADAR1}$ complex were not observed, even though the $f_Z$ became larger than 0.7 (Fig. 4).

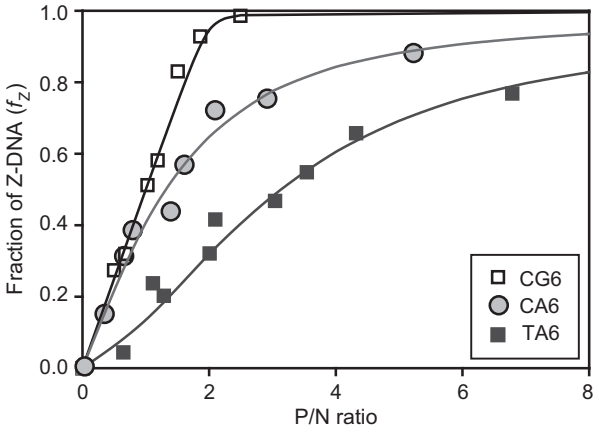


**Fig. 3.** The fraction of Z-DNA ($f_Z$) of CG6 (15) (open square, 35 °C), CA6 (gray circle, 25 °C) and TA6 (closed square, 15 °C) as a function of the $P/N$ ratio. Solid lines are simulated $f_Z$ of the DNA duplexes induced by $Z\alpha_{ADAR1}$.

### 3.3. Passive B–Z transition mechanism

In the *passive* B–Z transition mechanism (Fig. 1), the change of the $k_{ex}$ data for the G4z imino proton of CA6 and G2z imino proton of TA6 can be explained by the presence of mixtures of two imino protons from **ZP** and **ZP$_2$** in the imino peaks. In this case, the correlation between the observed $k_{ex}$ for the imino proton of the Z-conformation and the $f_Z$ is given by Eq. (2) (see Supplementary material):

$$k_{ex} = k_{ex}^{ZP2} + \frac{(k_{ex}^{ZP} - k_{ex}^{ZP2})}{2\gamma K_{BZ}^0 f_Z}\left\{\sqrt{(1-f_Z)^2 + 4\gamma K_{BZ}^0 f_Z(1-f_Z)} - 1 + f_Z\right\} \quad (2)$$

where $k_{ex}^{ZP}$ and $k_{ex}^{ZP2}$ are the $k_{ex}$ of the imino protons for **ZP** and **ZP$_2$**, respectively, $K_{BZ}^0 = [\mathbf{B}]/[\mathbf{Z}]$, and $\gamma$ $(= K_a^{ZP2}/K_a^{ZP})$ is the ratio of the association constants, $K_a$, of the **ZP$_2$** and **ZP** complex states. Unfortunately, no significant change in the $k_{ex}$ data for the G2z of TA6 and G4z of CA6 was observed under this experimental condition unlike the CG6 (Fig. 4C and D) and thus the *passive* B–Z transition model could not be evaluated in this system. The $k_{ex}$ data for the G2b of TA6 and G4b of CA6 should be uniform because the **BP** and **BP$_2$** complex states did not exist in this model. However, the strong dependence of $k_{ex}$ data for these imino protons on the $f_Z$ value

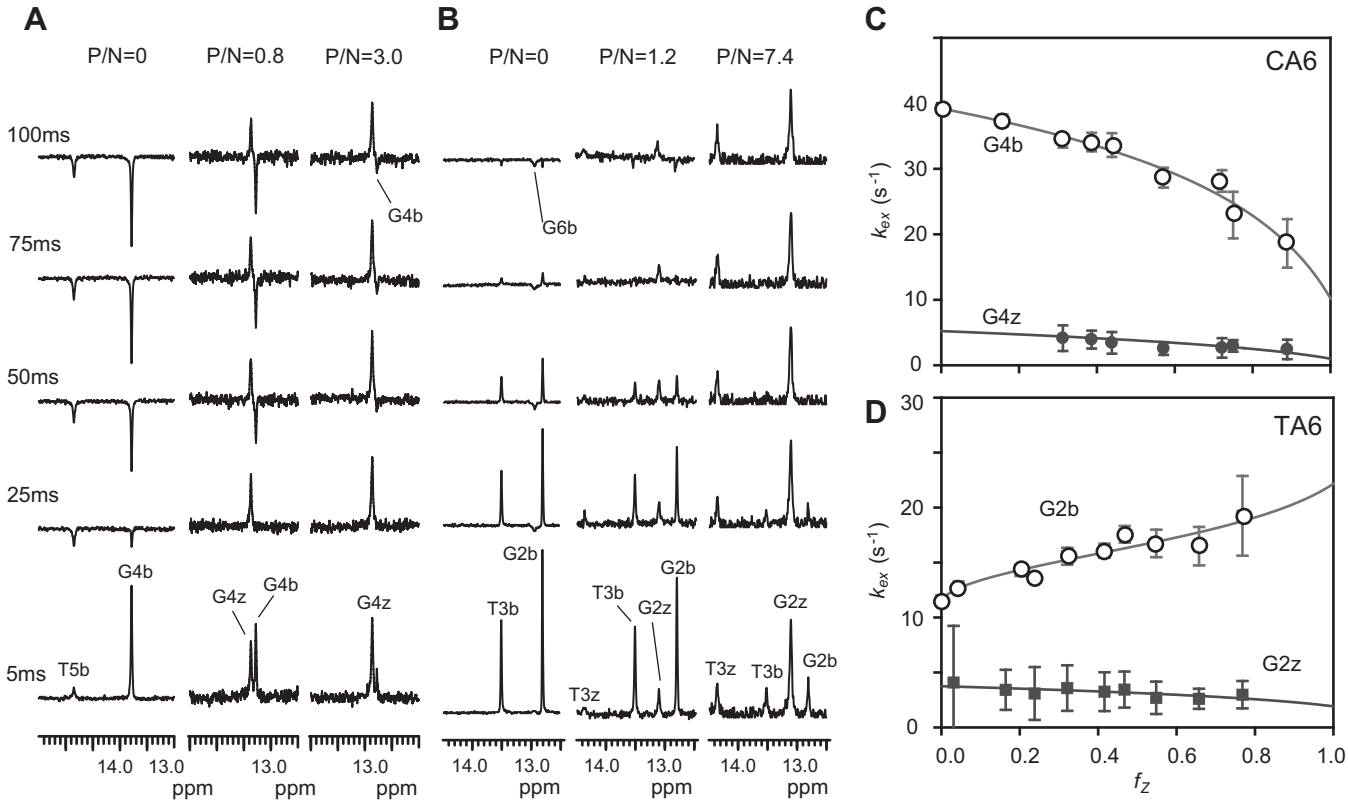


**Fig. 4.** (A) 1D imino proton spectra of the water magnetization transfer experiments for free CA6 (left) and CA6–Zα$_{ADAR1}$ complexes at the $P/N$ = 0.8 (middle) or 3.0 (right) at 25 °C. (B) 1D imino proton spectra of the water magnetization transfer experiments for free TA6 (left) and TA6–Zα$_{ADAR1}$ complexes at the $P/N$ = 1.2 (middle) or 7.4 (right) at 15 °C. The delay times between the selective water inversion and acquisition pulse are indicated on the left of spectra. (C) The $k_{ex}$ values of the G4b (open circle) and G4z (closed circle) imino protons for the CA6–Zα$_{ADAR1}$ complex determined at 25 °C and (D) $k_{ex}$ values of the G2b (open circle) and G2z (closed square) imino protons for the TA6–Zα$_{ADAR1}$ complex determined at 15 °C as a function of the $f_Z$. Solid lines are the best fit to Eq. (3), where the $k_{ex}$ data were weighted by the inverse of their variance.

(shown in Fig. 4C and D) means that the **BP** and/or **BP$_2$** complex states exist as intermediate during the Zα$_{ADAR1}$–induced B–Z transition of CA6 and TA6. Thus the *active* mechanism model should be considered to analyze the B–Z transition of the CA6 and TA6 duplexes induced by Zα$_{ADAR1}$, even though the *passive* B–Z transition model could not be evaluated.

### 3.4. Active B–Z transition mechanism

In the *active-mono* pathway of the *active* B–Z transition mechanism (Fig. 1), the change of the $k_{ex}$ data for the imino protons of the B-conformation can be explained by the presence of mixtures of two imino protons from **B** and **BP** in the imino peaks. In this case, the correlation between the observed $k_{ex}$ for the imino proton of the B-conformation and the $f_Z$ is given by Eq. (3) (see Supplementary material):

$$k_{ex} = k_{ex}^{B} + \frac{(k_{ex}^{BP} - k_{ex}^{B})}{2(1-\alpha)(1-f_Z)} \times \left\{ 1 + (K_{BZ}^{1} - 1)f_Z - \sqrt{(1 + (K_{BZ}^{1} - 1)f_Z)^2 - 4K_{BZ}^{1}(1-\alpha)f_Z(1-f_Z)} \right\} \quad (3)$$

where $k_{ex}^{B}$ and $k_{ex}^{BP}$ are the $k_{ex}$ of the imino protons for **B** and **BP**, respectively, $K_{BZ}^{1} = [\mathbf{BP}]/[\mathbf{ZP}]$, and $\alpha$ ($= K_a^{ZP2}/K_a^{BP}$) is the ratio of the association constants, $K_a$, of the **ZP$_2$** and **BP** complex states. The $\alpha$, $K_{BZ}^{1}$, and $k_{ex}^{BP}$ values of CA6 and TA6 complexed with Zα$_{ADAR1}$ were determined by curve fitting $k_{ex}$ of the imino protons as a function of $f_Z$ with Eq. (3) (Fig. 4C and D). The $k_{ex}^{BP}$ (10.2 $s^{-1}$) of the G4b in the CA6–Zα$_{ADAR1}$ complex was much smaller than its $k_{ex}^{B}$ value (39.2 $s^{-1}$) (Table 1). This result implies that the exchange process of the G4 imino proton might be reduced by Zα$_{ADAR1}$ bound to B-DNA. Interestingly, the $k_{ex}^{BP}$ value (22.2 $s^{-1}$) of the G2b imino proton in the TA6–Zα$_{ADAR1}$ complex was significantly larger than their $k_{ex}^{B}$ values (Table 1). These results mean that the TA6 duplex base pairs became unusually destabilized when Zα$_{ADAR1}$ bound to B-DNA, in contrast to the CA6 duplex base pairs. The $k_{ex}^{ZP}$ values for the imino protons for the Z-conformation could not be determined because these imino protons did not show any significant change in the $k_{ex}$ data (Fig. 4C and D).

It was previously reported that free CG6 exhibits only the B-form conformation when [NaCl] $\leqslant$ 1 M, but begins to transition to the Z-form when [NaCl] $\geqslant$ 2 M [15], suggesting that free DNA does not undergo the B–Z transition under physiolgical conditions (i.e. $K_{BZ}^{0} = [\mathbf{B}]/[\mathbf{Z}] \gg 1$). When the DNA is bound to one molecule of Zα$_{ADAR1}$, the B-form helix in the **BP** state could be easily converted to Z-DNA because $K_{BZ}^{1}$ for CG6 is about one [15]. Similarly, our study revealed that the CA6 B-DNA duplex ($K_{BZ}^{1} = 0.4 \pm 0.1$) is efficiently changed to Z-DNA by the binding of one molecule of Zα$_{ADAR1}$ via the *active-mono* mechanistic process, like CG6. However, the larger $K_{BZ}^{1}$ value (= 6.3 ± 3.1) of TA6 versus CG6 and CA6 means that the Zα$_{ADAR1}$-induced B–Z transition of TA6 via the *active-mono* pathway occurred less efficiently.

### 3.5. Association constants for the CA6–Zα$_{ADAR1}$ and TA6–Zα$_{ADAR1}$ complexes

The $\alpha$ values for the CA6–Zα$_{ADAR1}$ and TA6–Zα$_{ADAR1}$ complex are 1.42 and 13.9, respectively (Table 1). The concentrations of CA6 and TA6 complexed with Zα$_{ADAR1}$ at the various $P/N$ ratios were

**Table 1**
Exchange rate constants of the imino protons of different states of the DNA–Z$\alpha_{ADAR1}$ complexes and equilibrium constants for the Z$\alpha_{ADAR1}$-induced B–Z transition.

| Duplex | Imino | $k_{ex}^{B}$ ($s^{-1}$) | $k_{ex}^{BP}$ ($s^{-1}$) | $\alpha$[a] | $K_{BZ}^{1}$[b] | $K_a^B$ | $K_a^{ZP2}$ |
|---|---|---|---|---|---|---|---|
| CA6[c] | G4b | 39.2 ± 0.6 | 10.2 ± 3.1 | 1.42 | 0.4 ± 0.1 | $3.9 \pm 1.3 \times 10^3$ | $5.5 \pm 1.9 \times 10^3$ |
| TA6[d] | G2b | 11.5 ± 0.5 | 22.2 ± 5.3 | 13.9 | 6.3 ± 3.1 | $2.5 \pm 0.9 \times 10^3$ | $3.5 \pm 1.3 \times 10^4$ |

[a] $\alpha = K_a^{ZP2}/K_a^{BP}$.
[b] $K_{BZ}^{1} = [\mathbf{BP}]/[\mathbf{ZP}]$.
[c] Determined at 25 °C.
[d] Determined at 15 °C.

calculated as described in Supplementary material section (Tables S3 and S4). From these concentrations, the association constants for the CA6–Z$\alpha_{ADAR1}$ and TA6–Z$\alpha_{ADAR1}$ complexes were calculated (Supplementary material Tables S3 and S4), and their average values are shown in Table 1. The $K_a^{BP}$ values of CA6–Z$\alpha_{ADAR1}$ and TA6–Z$\alpha_{ADAR1}$ are $3.9 \pm 1.3 \times 10^3$ and $2.5 \pm 0.9 \times 10^3$, respectively. The $K_a^{ZP2}$ values of CA6–Z$\alpha_{ADAR1}$ and TA6–Z$\alpha_{ADAR1}$ are $5.5 \pm 1.9 \times 10^3$ and $3.5 \pm 1.3 \times 10^4$, respectively, indicating that the binding of the second Z$\alpha_{ADAR1}$ to the DNA duplex is slightly more efficient than the initial binding to the B-DNA. Interestingly, these $K_a^{BP}$ and $K_a^{ZP2}$ values are much smaller than those of CG6–Z$\alpha_{ADAR1}$ (>$10^7$). Crystal structural studies found that, in contrast to the behavior of CG6, some intermolecular hydrogen bonding interactions vanished in TA6 and CA6 complexed with Z$\alpha_{ADAR1}$ [4,21]. This structural feature could explain the lower binding affinities of Z$\alpha_{ADAR1}$ for the non-CG-repeat TA6 and CA6 duplexes as compared to CG6.

The B–Z transition induced by Z$\alpha_{ADAR1}$ was further evaluated by ITC. Fig. 5A presents the heat produced during titration of CG6 against Z$\alpha_{ADAR1}$ at 35 °C. Each addition of CG6 resulted in the release of heat until the binding was saturated (Fig. 5A). The CG6 data did not fit well with 'one-site binding (stoichiometric parameter $n = 2$)' model or 'two sequential binding' model but suggested a 'two-site binding' model. However, two stoichiometric parameters in the two-site binding model were larger than one. This behavior may result from the B–Z transition step which could not be considered in any ITC binding model. This analysis produced the binding parameters: $K_{a1} = 3.9 \times 10^7$, $K_{a2} = 3.2 \times 10^5$, $\Delta H_1 = -3.7$ kcal/mol, $\Delta H_2 = -1.2$ kcal/mol, $T\Delta S_1 = -4.0$ kcal/mol, $T\Delta S_2 = -9.6$ kcal/mol, and $\Delta G^o_{overall} = \Delta G^o_1 + \Delta G^o_2 = -18.4$ kcal/mol. Contrast to CG6, each addition of CA6 at 25 °C or TA6 at 15 °C resulted in the absorption of heat (Fig. 5B and C), which indicates that the binding of Z$\alpha_{ADAR1}$ to CA6 and TA6 is an endothermic process ($\Delta H > 0$). The calculated $\Delta G^o_{overall}$ values for binding of Z$\alpha_{ADAR1}$ to CA6 (25 °C) and TA6 (25 °C) are −12.2 and −11.3 kcal/mol, respectively. Even though these $\Delta G^o_{overall}$ values cannot be used because this analysis did not consider the B–Z transition step, the ITC results clearly supported the DNA sequence-dependent B–Z transition mechanism (see Fig. 6) studied by NMR spectroscopy.

### 3.6. Implication for DNA sequence discrimination of Z$\alpha_{ADAR1}$

Fig. 6 shows the diagram for Gibbs free energies of the mechanism for the B–Z transition induced by Z$\alpha_{ADAR1}$, which were calculated from association constants using the equation $\Delta G^o = -RT\ln K_a$. This figure can explain how Z$\alpha_{ADAR1}$ exhibits the sequence preference of CG6 ≫ CA6 > TA6 during the B–Z transition. First, the **P** binds to the **B**, with a sequence preference of CG6 ≫ CA6 > TA6, even though the structural features of these three DNA duplexes complexed with Z$\alpha_{ADAR1}$ are very similar to each other. This distinct difference in the binding affinities for the different DNA duplexes is the first sequence discrimination factor of Z$\alpha_{ADAR1}$ during the B–Z transition. Second, the **BP** of CG6 and CA6 convert to **ZP**, whereas this process occurs less efficiently in for TA6. These different B–Z transition activities allow Z$\alpha_{ADAR1}$ to discriminate

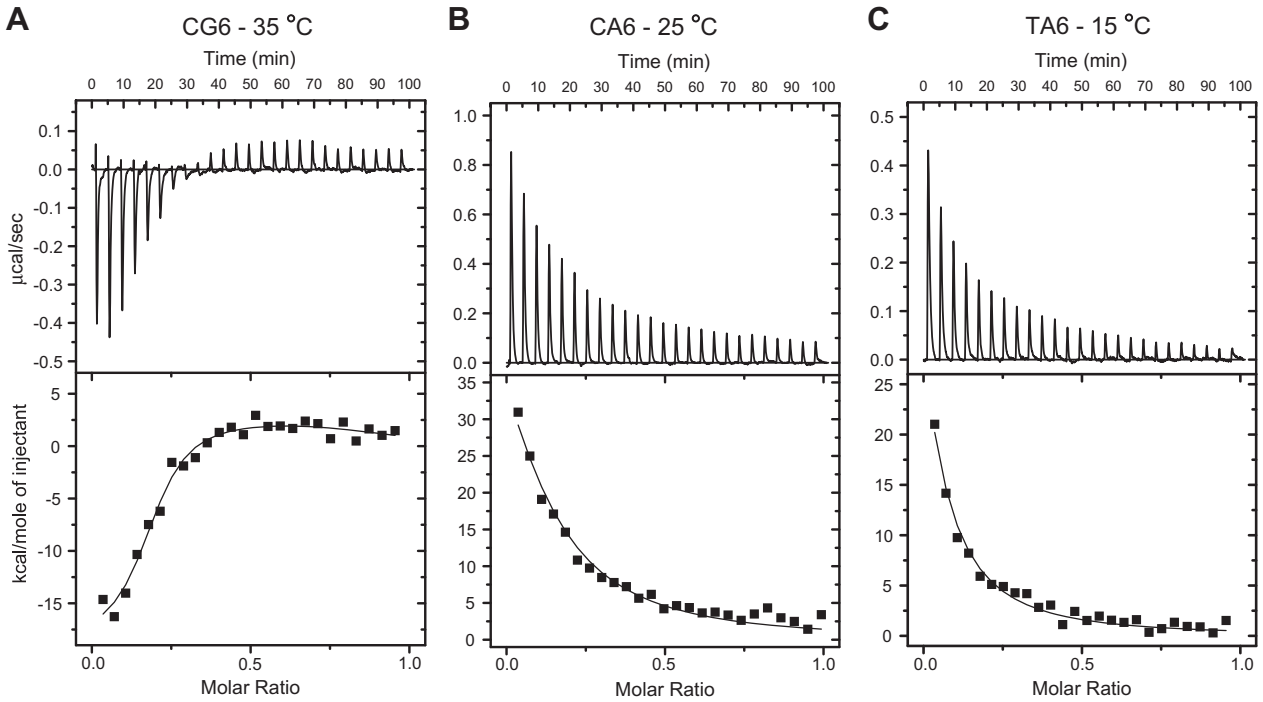


**Fig. 5.** ITC titration data for the binding of Z$\alpha_{ADAR1}$ with (A) CG6 (35 °C), (B) CA6 (25 °C), and (C) TA6 (15 °C) duplexes. Molar ratio indicates the DNA-to-protein molar ratio (inverse of the $P/N$ ratio). Solid lines represent the non-linear least-square best fitting with a two-site binding model.

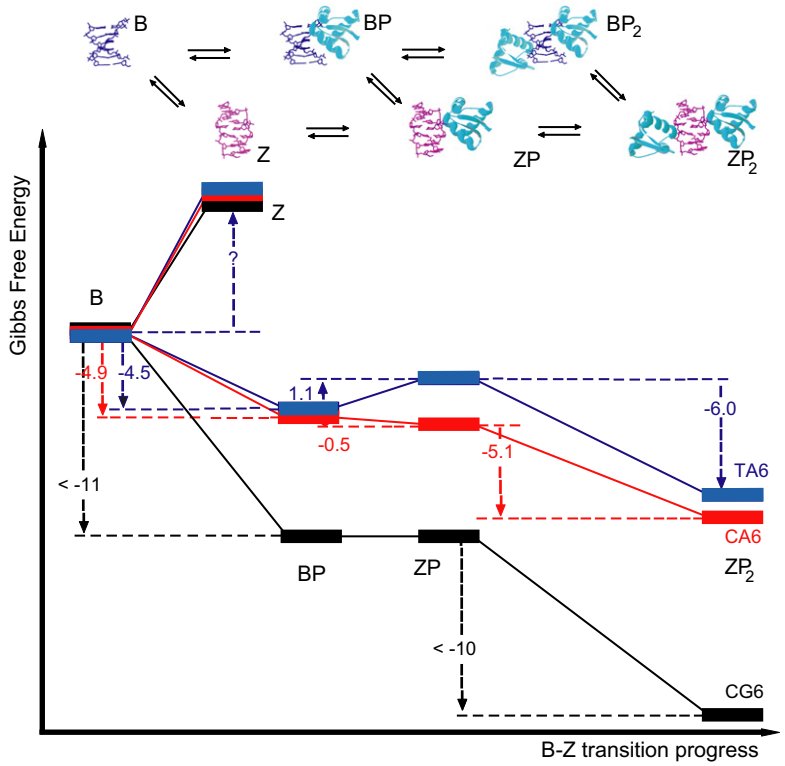


**Fig. 6.** Schematic representations of the possible Gibbs energy diagram of the $Z\alpha_{ADAR1}$ binding and B–Z transition of the CG6 [35 °C, black, previous study (15)], CA6 (25 °C, red), and TA6 (15 °C, blue) duplexes. Gibbs free energies (kcal/mol) for reaction steps were calculated using the equation, $\Delta G^{o} = -RT\ln K_a$.

d(TA)-containing DNA sequences from alternating pyrimidine–purine sequences. Third, the **ZP** of CG6 and CA6 binds to the **P** and forms the stable **$ZP_2$** complex with a sequence preference of CG6 ≫ CA6, which might act as the third sequence discrimination step. Taken together, we can propose the new model that $Z\alpha_{ADAR1}$ selectively recognizes the alternating $d(CG)_n$ sequence and then converts it to Z-form helix in a long genomic DNA through its multiple sequence discrimination steps.

## 4. Conclusions

Our study suggests that $Z\alpha_{ADAR1}$ binds to Z-DNA via an *active* B–Z transition mechanism in which $Z\alpha_{ADAR1}$ first binds to B-DNA and then converts it to left-handed Z-DNA that is stabilized by the binding of a second $Z\alpha_{ADAR1}$ molecule. During the B–Z transition, $Z\alpha_{ADAR1}$ exhibits the sequence preference of $d(CGCGCG)_2 \gg d(CACGTG)_2 > d(CGTACG)_2$ through multiple sequence discrimination steps. These results can explain how $Z\alpha_{ADAR1}$ selectively recognizes the alternating $(CG)_n$ sequence in a long genomic DNA.

## Acknowledgements

We thank Drs. Kyeong Kyu Kim and Yang-Gyun Kim for valuable comments on the manuscript. This work was supported by the National Research Foundation of Korea (NRF) Grants (2010-0014199, NRF-C1ABA001-2010-0020480, R01-2007-000-10691-0, KRF-2008-331-C00178 to J.-H.L.; 2009-0092818, 2009-220-C00036 to B.-S.C.; R15-2003-012-01001-0 to EB-NCRC) funded by Korean Government (MEST). We thank the KIST NMR facility for performing NMR experiment.

## Appendix A. Supplementary data

Supplementary data associated with this article can be found, in the online version, at doi:10.1016/j.febslet.2010.09.036.

## References

[1] Rich, A., Nordheim, A. and Wang, A.H. (1984) The chemistry and biology of left-handed Z-DNA. Annu. Rev. Biochem. 53, 791–846.
[2] Herbert, A. and Rich, A. (1996) The biology of left-handed Z-DNA. J. Biol. Chem. 271, 11595–11598.
[3] Herbert, A. and Rich, A. (1999) Left-handed Z-DNA: structure and function. Genetica 106, 37–47.
[4] Schwartz, T., Rould, M.A., Lowenhaupt, K., Herbert, A. and Rich, A. (1999) Crystal structure of the Zα domain of the human editing enzyme ADAR1 bound to left-handed Z-DNA. Science 284, 1841–1845.
[5] Schwartz, T., Behlke, J., Lowenhaupt, K., Heinemann, U. and Rich, A. (2001) Structure of the DLM-1-Z-DNA complex reveals a conserved family of Z-DNA-binding proteins. Nat. Struct. Biol. 8, 761–765.
[6] Ha, S.C., Lokanath, N.K., Van Quyen, D., Wu, C.A., Lowenhaupt, K., Rich, A., Kim, Y.G. and Kim, K.K. (2004) A poxvirus protein forms a complex with left-handed Z-DNA: crystal structure of a Yatapoxvirus Zα bound to DNA. Proc. Natl. Acad. Sci. USA 101, 14367–14372.
[7] Kahmann, J.D. et al. (2004) The solution structure of the N-terminal domain of E3L shows a tyrosine conformation that may explain its reduced affinity to Z-DNA in vitro. Proc. Natl. Acad. Sci. USA 101, 2712–2717.
[8] Ha, S.C., Lowenhaupt, K., Rich, A., Kim, Y.G. and Kim, K.K. (2005) Crystal structure of a junction between B-DNA and Z-DNA reveals two extruded bases. Nature 437, 1183–1186.
[9] Athanasiadis, A., Placido, D., Maas, S., Brown 2nd, B.A., Lowenhaupt, K. and Rich, A. (2005) The crystal structure of the Zβ domain of the RNA-editing enzyme ADAR1 reveals distinct conserved surfaces among Z-domains. J. Mol. Biol. 351, 496–507.
[10] Ha, S.C., Kim, D., Hwang, H.Y., Rich, A., Kim, Y.G. and Kim, K.K. (2008) The crystal structure of the second Z-DNA binding domain of human DAI (ZBP1) in complex with Z-DNA reveals an unusual binding mode to Z-DNA. Proc. Natl. Acad. Sci. USA 105, 20671–20676.
[11] Brown 2nd, B.A. and Rich, A. (2001) The left-handed double helical nucleic acids. Acta Biochim. Pol. 48, 295–312.
[12] Herbert, A.G. and Rich, A. (1993) A method to identify and characterize Z-DNA binding proteins using a linear oligodeoxynucleotide. Nucleic Acids Res. 21, 2669–2672.
[13] Herbert, A., Alfken, J., Kim, Y.G., Mian, I.S., Nishikura, K. and Rich, A. (1997) A Z-DNA binding domain present in the human editing enzyme, double-stranded RNA adenosine deaminase. Proc. Natl. Acad. Sci. USA 94, 8421–8426.
[14] Herbert, A., Schade, M., Lowenhaupt, K., Alfken, J., Schwartz, T., Shlyakhtenko, L.S., Lyubchenko, Y.L. and Rich, A. (1998) The Zα domain from human ADAR1 binds to the Z-DNA conformer of many different sequences. Nucleic Acids Res. 26, 3486–3493.

[15] Kang, Y.-M. et al. (2009) NMR spectroscopic elucidation of the B–Z transition of a DNA double helix induced by the Zα domain of human ADAR1. J. Am. Chem. Soc. 131, 11485–11491.
[16] Wang, A.H., Hakoshima, T., van der Marel, G., van Boom, J.H. and Rich, A. (1984) A·T base pairs are less stable than G·C base pairs in Z-DNA: the crystal structure of d($m^5$CGTA$m^5$CG). Cell 37, 321–331.
[17] Coll, M., Fita, I., Lloveras, J., Subirana, J.A., Bardella, F., Huynh-Dinh, T. and Igolen, J. (1988) Structure of d(CACGTG), a Z-DNA hexamer containing A·T base pairs. Nucleic Acids Res. 16, 8695–8705.
[18] Eichman, B.F., Schroth, G.P., Basham, B.E. and Ho, P.S. (1999) The intrinsic structure and stability of out-of-alternation base pairs in Z-DNA. Nucleic Acids Res. 27, 543–550.
[19] McLean, M.J., Blaho, J.A., Kilpatrick, M.W. and Wells, R.D. (1986) Consecutive A·T pairs can adopt a left-handed DNA structure. Proc. Natl. Acad. Sci. USA 83, 5884–5888.
[20] Ellison, M.J., Feigon, J., Kelleher 3rd, R.J., Wang, A.H., Habener, J.F. and Rich, A. (1986) An assessment of the Z-DNA forming potential of alternating dA–dT stretches in supercoiled plasmids. Biochemistry 25, 3648–3655.
[21] Ha, S.C., Choi, J., Hwang, H.Y., Rich, A., Kim, Y.G. and Kim, K.K. (2009) The structures of non-CG-repeat Z-DNAs co-crystallized with the Z-DNA-binding domain, hZ$\alpha_{ADAR1}$. Nucleic Acids Res. 37, 629–637.
[22] Delaglio, F., Grzesiek, S., Vuister, G.W., Zhu, G., Pfeifer, J. and Bax, A. (1995) NMRPipe: a multidimensional spectral processing system based on UNIX pipes. J. Biomol. NMR 6, 277–293.
[23] Goddard, T.D. and Kneller, D.G. (2003) SPARKY 3, University of California, San Francisco, CA.
[24] Lee, J.-H. and Pardi, A. (2007) Thermodynamics and kinetics for base-pair opening in the P1 duplex of the *Tetrahymena* group I ribozyme. Nucleic Acids Res. 35, 2965–2974.
[25] Lee, J.-H., Jucker, F. and Pardi, A. (2008) Imino proton exchange rates imply an induced-fit binding mechanism for the $VEGF_{165}$-targeting aptamer, Macugen. FEBS Lett. 582, 1835–1839.
[26] Gueron, M. and Leroy, J.L. (1995) Studies of base pair kinetics by NMR measurement of proton exchange. Methods Enzymol. 261, 383–413.
[27] Bang, J., Bae, S.-H., Park, C.-J., Lee, J.-H. and Choi, B.-S. (2008) Structural and dynamics study of DNA dodecamer duplexes that contain un-, hemi-, or fully methylated GATC sites. J. Am. Chem. Soc. 130, 17688–17696.
[28] Bang, J., Kang, Y.-M., Park, C.-J., Lee, J.-H. and Choi, B.-S. (2009) Thermodynamics and kinetics for base pair opening in the DNA decamer duplexes containing cyclobutane pyrimidine dimer. FEBS Lett. 583, 2037–2041.